frontiers | Frontiers in Earth Science

TYPE Original Research
PUBLISHED 12 September 2022
DOI 10.3389/feart.2022.959602

OPEN ACCESS

EDITED BY
Dongming Zhi,
PetroChina, China

REVIEWED BY
Xiaoqi Wu,
SINOPEC Petroleum Exploration and Production Research Institute, China
Pingping Li,
China University of Petroleum, China

*CORRESPONDENCE
Fanghao Xu,
13618043318@163.com

SPECIALTY SECTION
This article was submitted to Economic Geology, a section of the journal Frontiers in Earth Science

RECEIVED 01 June 2022
ACCEPTED 20 July 2022
PUBLISHED 12 September 2022

CITATION
Xiao H, Xu F, Fu X, Li W, Chen C, Zhang J, Wang Y and Zhou K (2022), Main factors controlling hydrocarbon accumulation in the Northwestern Sichuan Basin. *Front. Earth Sci.* 10:959602. doi: 10.3389/feart.2022.959602

Main factors controlling hydrocarbon accumulation in the Northwestern Sichuan Basin

Hang Xiao[1], Fanghao Xu[1]*, Xiaodong Fu[2], Wenzheng Li[2], Cong Chen[3], Jianyong Zhang[2], Yajie Wang[1,4] and Kuan Zhou[1]

[1]State Key Laboratory of Oil and Gas Reservoir Geology and Exploitation, Chengdu University of Technology, Chengdu, China, [2]Hangzhou Institute of Geology, PetroChina, Hangzhou, China, [3]PetroChina Southwest Oil and Gas Field Company, Chengdu, China, [4]Overseas Business Department, Geophysical Research Institute, Bureau of Geophysical Prospecting, CNPC, Zhuozhou, China

The basin-mountain transition regions of foreland basins are hot spots for hydrocarbon exploration worldwide, while the complex geological features and hydrocarbon accumulation rules make hydrocarbon exploration very difficult. The Northwestern Sichuan Basin is a typical case where the unclear distribution rules restrict the further exploration of natural gas. In this study, geochemistry and seismic profile data were comprehensively used to reveal the main factors controlling hydrocarbon accumulation in the Northwestern Sichuan Basin. The Lower Cambrian and the Upper- Middle Permian source rocks have different carbon isotope compositions, indicating that they have different kerogen types, sapropelic kerogen for the Lower Cambrian source rocks, mixed kerogen for the Middle Permian source rocks and humic kerogen for the Upper Permian source rocks. The Northwestern Sichuan Basin can be divided into the unfaulted belt, the thrust front belt and the thrust nappe belt. The thrust nappe belt develops many large thrust faults, and the natural gas there mainly originates from the Lower Cambrian source rocks. However, due to different denudation of regional caprocks, hydrocarbons in the area adjacent to the Longmen Mountain fold-and-thrust system were destroyed, while in the area adjacent to the thrust front belt, they had good preservation conditions. The thrust front belt and the unfaulted belt develop a few or few thrust faults, and the natural gas there mainly originates from the Upper-Middle Permian source rocks and has good preservation conditions due to no denudation of regional caprocks. The distribution of thrust faults controls the natural gas origins in different areas, and the preservation conditions determine whether the gas reservoirs can survive to the present. These conclusions can provide guidance for natural gas exploration in the Northwestern Sichuan Basin and other basin-mountain transition regions in foreland basins worldwide.

KEYWORDS

foreland basin, basin-mountain transition regions, gas source correlation, hydrocarbon accumulation process, carbon isotope

1 Introduction

The basin-mountain transition regions of the foreland basins have favorable hydrocarbon accumulation conditions and are regarded as hot spots for hydrocarbon exploration worldwide (Wei et al., 2019; Wei et al., 2020). Many large oil or gas fields have been discovered there, such as the Pineview oil field in the western Green River Basin of the United States (Deming and Chapman, 1988), the Chemchemal gas field in the Zagross Fold Belt of North Iraq (Al-ameri and Zumberge, 2012) and the Alade oilfield in the Northwestern Junggar Basin of China (Guo et al., 2021). However, these regions are characterized by intense tectonic movement, complex geological evolution and intricate hydrocarbon accumulation processes, which make hydrocarbon exploration very difficult (Decelles and Gilest, 1996; Macclay, 2004; He and Jia, 2005; Picha, 2011; Guo et al., 2020).

The Sichuan Basin is a large superimposed basin with abundant hydrocarbon resources, and its Northwestern region (the Northwestern Sichuan Basin) is a typical basin-mountain transition region between the Longmen Mountain and the eastern foreland basin. The Northwestern Sichuan Basin has a long history of natural gas exploration dating back to the 1970s. At that time, under the guidance of the traditional exploration idea that hydrocarbon exploration should be at the structural high point, some exploration wells were drilled in the hanging wall of the thrust nappe belt, such as the Kuangshanliang area, but there were no major exploration breakthroughs except for very few wells with high production of natural gas. However, exploration wells drilled in the Shuangyushi area of the thrust front belt have achieved major success, indicating huge natural gas exploration prospects in the thrust front belt. This suggests that complex and various hydrocarbon accumulation rules exist in different regions of the Northwestern Sichuan Basin, which restricts the further exploration of natural gas. Determining the major factors controlling natural gas accumulation is the key to subsequent natural gas exploration in the Northwestern Sichuan Basin.

On the basis of research on the chemical composition of natural gas, carbon isotope features of source rocks and natural gas, and geological feature differences between different regions in the Northwestern Sichuan Basin, this paper attempts to 1) determine the genesis and origins of natural gas in different regions; 2) clarify the hydrocarbon accumulation process in the Northwestern Sichuan Basin; and 3) explore the main factors controlling natural gas accumulation in the Northwestern Sichuan Basin.

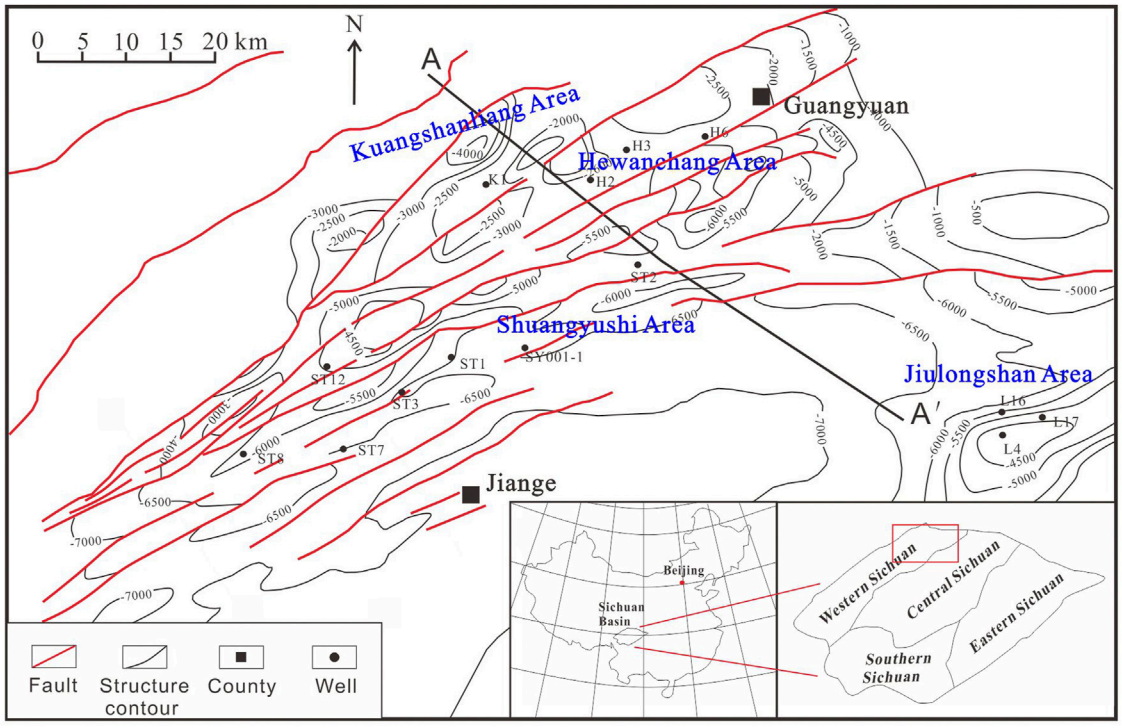

FIGURE 1
Regional position of the Northwestern Sichuan Basin. Note the top structure contours of the Qixia Formation.

2 Geological setting

The Sichuan Basin, located in southwestern China (Figure 1), is a large and petroliferous basin, with total natural gas reserves of approximately 53477.4×10^8 m^3 (Li B. et al., 2020). It has proven reserves of 16497.52×10^8 m^3 and has tremendous potential for natural gas exploration (Li B. et al., 2020). The Sichuan Basin is bounded by the Longmen Mountain orogenic belt to the northwest, the Micanshan uplift and Daba Mountain thrust belt to the northeast, and the Hunan-Guizhou-Hubei fold belt to the southeast (Wu et al., 2021). The Northwestern Sichuan Basin is located at the intersection of the Micangshan uplift belt and the Longmen Mountain fault-fold belt and consists of Wangcang, Jiange, Guanyuan and Cangxi counties.

The Northwestern Sichuan Basin experienced two tectonic stages: the craton basin stage (Neoproterozoic to early Mesozoic) and the foreland basin stage (middle Mesozoic to the present) (Chen X. Z. et al., 2019). The superimposed stratigraphic sequences were developed in the Northwestern Sichuan Basin and mainly consist of marine deposits from the Sinian to the Middle Triassic and continental deposits from the Upper Triassic to the present (Figure 2) (Li et al., 2022; Miao et al., 2022). The Lower Cambrian shales, the Upper-Middle Permian coal measures and marlstones, and the Upper Triassic shales are the main source rocks, while the Sinian and Paleozoic carbonate rocks and the Devonian and Mesozoic sandstones are good reservoirs for hydrocarbons (Figure 2) (Chen X. Z. et al., 2019; Li W. et al., 2020; Deng et al., 2022; Miao et al., 2022).

The Northwestern Sichuan Basin has experienced multiple tectonic events, such as the Emei Taphrogeny, Indo–Yanshanian orogeny and Himalayan orogeny (Wang et al., 2018; Xiao et al., 2021). During the Indo–Yanshanian orogeny, the Northwestern Sichuan Basin became a foredeep basin, and during the Himalayan orogeny, affected by the Longmen Mountain fold-and-thrust system, the Northwestern Sichuan Basin can be divided into three structural belts: the unfaulted belt, the thrust front belt and the thrust nappe belt (Figure 3) (Xiao et al., 2021; Li et al., 2022). The Hewanchang, Shuangyushi, Jiulongshan and Kuangshanliang areas are important gas-bearing structures in the Northwestern Sichuan Basin. The Kuangshanliang and Hewanchang areas are located in the thrust nappe belt, the Shuangyushi area is located in the thrust front belt, and the Jiulongshan area is located in the unfaulted belt (Figure 1).

The Qiongzhusi Formation ($\in_1$q) in the Lower Cambrian, the Qixia (P_2q) and Maokou (P_2m) formations in the Middle Permian and the Longtan Fomation (P_3l) in the Upper Permian develop the major source rocks for the Palaeozoic reservoirs in the Northwestern Sichuan Basin (Figure 2) (Hu et al., 2021; Xiao et al., 2021). The$\in_1$q source rocks are black, dark gray marine shale, and the P_2q and P_2m source rocks are gray black marine marlstones. The P_3l source rocks are black coal measures. The P_2q and P_2m also develop the most important reservoirs for natural gas in the Northwestern Sichuan Basin (Figure 2). P_2q is mainly composed of platform margin beach deposits, with the main lithology of brown–gray, light gray fine/mesocrystalline dolomite and medium/coarse-crystalline dolomite. The porosity and permeability of the P_2q reservoirs range from 0.42 to 16.51% (avg. 3.58%) and from 1.51 mD to 784 mD (avg. 10.9 mD), respectively (Chen C. et al., 2019). P_2m mainly consists of the deposits of platform margin beach and gentle slope. The natural gas reservoirs in P_2m can be divided into two kinds: limestone fracture-type reservoirs deposited in gentle slope facies and dolomite pore-type reservoirs deposited in platform margin beach facies (Huo et al., 2018). The former mainly belong to reservoirs with ultralow porosity and low permeability, while the latter mainly belong to reservoirs with medium porosity and medium permeability (Huo et al., 2018).

3 Samples and analytical methods

Twenty-one source rock samples from the Lower Cambrian and the Upper-Middle Permian of the Northwestern Sichuan Basin were selected for the carbon isotopic test. Seven natural gas samples from the Qixia Formation in the Shuangyushi area were selected for analyzing the chemical compositions. Six natural gas samples from the Hewanchang area and fifteen natural gas samples from the Shuangyushi area were also collected for the carbon isotopic test.

The carbon isotopic composition of the source rock samples was determined on a Finnigan Delta Plus mass spectrometer. The source rock samples were combusted at 1000°C to generate carbon dioxide after decalcification, which was used to determine the carbon isotopic composition of organic matter. The carbon isotopic compositions were reported in the δ notation in per mil (‰) relative to the VPDB standard, and the accuracy for the measurement was ±0.1‰.

The Chemical composition of the natural gas samples was analyzed by a Hewlett Packard 6890 II gas chromatograph equipped with a flame ionization detector and a thermal conductivity detector. The gaseous alkanes were separated by using a capillary column (PLOT Al_2O_3 50 m × 0.53 mm). The GC oven temperature was initially set to 30°C for 5 min, then programmed to increase to 180°C at 10°C/min, and finally kept at 180°C for 10 min.

The carbon isotopic composition of gaseous alkanes was determined on a Finnigan MAT-253 mass spectrometer. The gaseous alkanes were separated through a fused silica capillary column (PLOT Q 30 m × 0.32 mm). Helium was used as the carrier gas. The GC oven temperature was programmed to 160°C increasing from 40°C at 10°C/min and finally kept at 160°C for 10 min. The natural gas samples were measured in triplicate, and the carbon isotopic compositions were reported in the δ notation in per mil (‰) relative to the VPDB standard. The accuracy for the measurement was ±0.5‰.

10.3389/feart.2022.959602

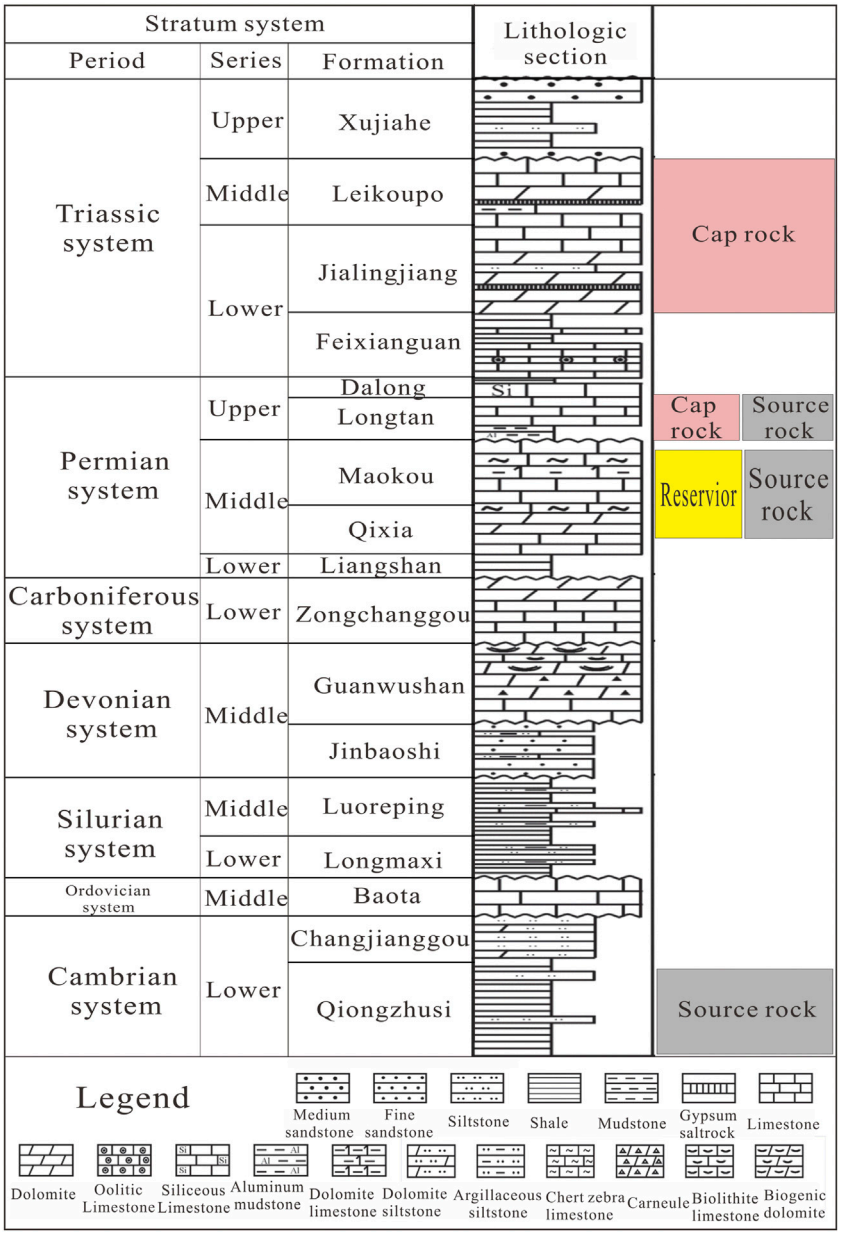

FIGURE 2
A generalized stratigraphic column of the Northwestern Sichuan Basin.

4 Results

4.1 Differences in geological features between different regions

Due to the distance from the Longmen Mountain fold-and-thrust system increasing from the thrust nappe belt to the thrust front belt and the unfaulted belt, the tectonic stress gradually decreases in the same order. Various tectonic stresses cause the above three regions to have different geological features, mainly in the distribution of thrust faults and the uplift of formations (Figure 3).

The thrust nappe belt is closest to the Longmen Mountain fold-and-thrust system and experiences the most intense tectonic stress. Therefore, under the influence of such intense tectonic stress, the strata uplifted violently, and many large thrust faults developed in the thrust nappe belt (Figure 3). Note that the denudation of strata varied in different areas, and the closer to the

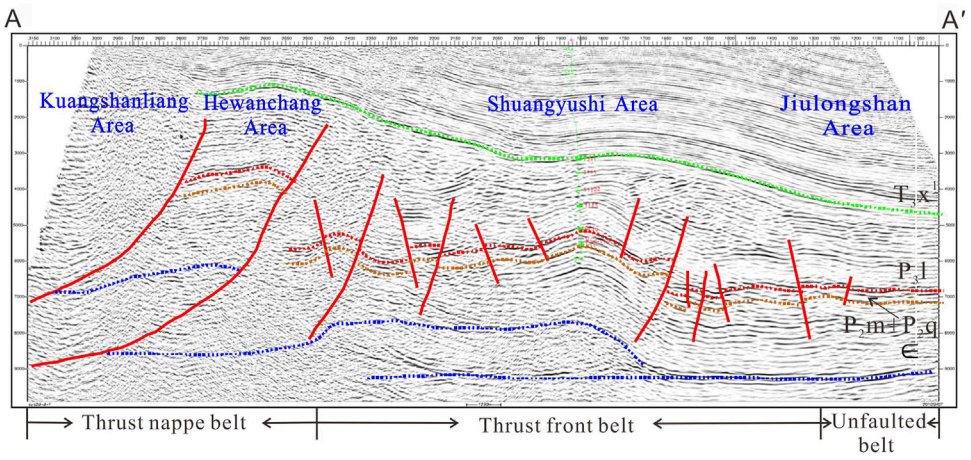

FIGURE 3
A seismic profile in the NW direction of the Northwestern Sichuan Basin to show the distribution of thrust faults and the uplift of formations in different areas Figure 1 for profile location.

Longmen Mountain fold-and-thrust system, the more serious denudation the strata suffered. The thrust front belt is farther from the orogenic belt than the thrust nappe belt, so tectonic stress there turned relatively weak. Therefore, the stratum experienced little or no uplift and denudation, and only a few thrust faults developed in the thrust front belt (Figure 3). The unfaulted belt is furthest from the orogenic belt and suffered the weakest tectonic stress, under the influence of which the unfaulted belt became a low hump and few thrust faults developed there (Figure 3).

4.2 Chemical composition of natural gas

The Chemical composition of natural gas from different regions in the Northwestern Sichuan Basin is shown in Table 1. The natural gas in the P_2q Formation of the Shuangyushi area are typical dry gas with gas dryness [$C_1/\Sigma(C_1–C_5)$] greater than 0.95%. The ethane content ranges from 0.10 to 0.11%, with an average of 0.11%. CO_2 is the most abundant nonhydrocarbon gas, with the average content of 1.24%. The content of H_2S is very low, with the gas souring index [GSI = 100 × $H_2S/(H_2S + CH_4 + C_2H_6 + C_3H_8)$] (Worden et al., 1995) values ranging from 0 to 0.008.

The natural gas in the P_2m Formation of the Hewanchang area are also typical dry gas. The ethane content is relatively high, ranging from 0.19 to 1.32%, with an average of 0.73%. N_2 is the most abundant nonhydrocarbon gas, with an average content of 1.16%. The content of H_2S is also very low, with GSI values ranging from 0 to 0.003.

The natural gas in the P_2m and P_2q Formations of the Jiulongshan area are typical dry gas as well, with ethane contents ranging from 0.1 to 0.94% (avg. 0.25%). N_2 is also the most abundant nonhydrocarbon, avg. 0.98%. H_2S has low content, with GSI values ranging from 0 to 0.009.

4.3 Carbon isotopic composition of source rocks and natural gas

The carbon isotopic compositions of source rocks from different stratigraphic intervals are shown in Table 2. The $\delta^{13}C$ values of the Lower Cambrian source rocks range from −38.8‰ to −34.9‰, avg. −36.5‰. The $\delta^{13}C$ values of the Middle Permian source rocks are larger than those of the Cambrian source rocks, ranging from −29.2‰ to −24.2‰, with an average of −26.9‰. The $\delta^{13}C$ values of the Upper Permian source rocks have the largest $\delta^{13}C$ values, ranging from −26.1‰ to −24.8‰, with an average of −25.4‰.

The carbon isotopic composition of natural gas from different areas is shown in Table 1. The $\delta^{13}C_1$ and $\delta^{13}C_2$ values of the natural gas samples from the Hewanchang area range from −36.7‰ to −32.9‰ (avg. −35.1‰) and from −36.7‰ to −32.5‰ (avg. −34.3‰), respectively. The natural gas samples from the Shuangyushi area have larger $\delta^{13}C_1$ and $\delta^{13}C_2$ values, ranging from −32.5‰ to −29.7‰ (avg. −30.5‰) and from −28.6‰ to −25.9‰ (avg. −27.3‰), respectively. The natural gas samples from the Jiulongshan area have $\delta^{13}C_1$ and $\delta^{13}C_2$ values ranging from −28.8‰ to −27.3‰ (avg. −28.2‰) and from −29.3‰ to −25.2‰ (avg. −27.3‰), respectively.

TABLE 1 Compositions and carbon isotopes of natural gas samples from different areas.

Area	Wactell	Strata	Hydrocarbon gases/%		Non-hydrocarbon gases/%					GSI	$\delta^{13}C_1$/‰	$\delta^{13}C_2$/‰	Data source
			CH_4	C_2H_6	N_2	CO_2	He	H_2	H_2S				
Shuangyushi	ST12	P_2q	96.56	0.11	0.85	1.71	0.03	0	0.74	0.008	−29.7	−26.8	This study
	SY132	P_2q	96.72	0.11	1.09	1.68	0.02	0	0.37	0.004	−30.4	−27.2	
	ST1	P_2q	96.65	0.1	0.87	2	0.03	0	0.34	0.004	−30.1	−28.2	
	ST3	P_2q	96.81	0.1	0.8	1.87	0.02	0.01	0.39	0.004	−30.5	−28.5	
	SY001-1	P_2q	97.14	0.11	0.95	1.4	0.02	0	0.38	0.004	−29.8	−28	
	ST7	P_2q	97.53	0.11	0	0	0.47	1.45	0.02	0.0002	−30.0	−27.1	
	ST8	P_2q	97.18	0.1	0	0	0.52	1.77	0.02	0.0002	−29.9	−26.7	
	ST1	P_2m	-	-	-	-	-	-	-	-	−32.5	−26.2	
	ST1	P_2m	-	-	-	-	-	-	-	-	−30.3	−26.3	
	ST1	P_2m	-	-	-	-	-	-	-	-	−30.2	−26.1	
	ST3	D_2g	-	-	-	-	-	-	-	-	−32.3	−28.6	
	ST3	D_2g	-	-	-	-	-	-	-	-	−31.1	−27.9	
	ST12	P_2q	-	-	-	-	-	-	-	-	−31.0	−25.9	
	ST12	P_2q	-	-	-	-	-	-	-	-	−30	−28.4	
	ST12	P_2q	-	-	-	-	-	-	-	-	−29.9	−28.2	
Hewanchang	H2	P_2m	-	-	-	-	-	-	-	-	−36.7	−32.8	
	H2	P_2m	-	-	-	-	-	-	-	-	−35.5	−33.4	
	H2	P_2m	-	-	-	-	-	-	-	-	−-32.9	−32.5	
	H3	O	-	-	-	-	-	-	-	-	−35.6	−36.7	
	H3	P_2ch	-	-	-	-	-	-	-	-	−35.3	−35.2	
	H3	O	-	-	-	-	-	-	-	-	−35.7	−36.4	
	H2	P_2m	97.08	0.65	1.7	0.36	0.04	0.01	0.05	0.001	−35.7	−33.4	Xiao et al. (2021)
	H2	P_2m	97.21	0	1.27	0.06	0.03	0.14	0	0	−33.7	-	
	H2	P_2m	96.01	1.32	1.43	0.21	0.05	0.13	0	0	−34.5	−34.7	
	H2	P_2m	97.67	0.69	1.38	0.06	0	0.16	0.05	0.001	−35.5	−33.6	
	H3	P_2m	97.82	0.56	1.18	0.33	1.18	0	0.05	0.001	−35.5	-	
	H6	P_2m	98.28	0.97	0.37	0.07	0.37	0.23	0	0	-	-	
	K1	P_2m	95.22	0.19	0.48	3.79	0.48	0	0.3	0.003	-	-	
Jiulongshan	LT1	P_2q	96.22	0.15	1.02	1.69	0.02	0.01	0.88	0.009	−28.8	−27.3	
	L004-X1	P_2m	98.1	0.14	0.72	0.48	0.02	0.01	0.54	0.005	27.3	−28.2	
	L004-X1	P_2m	96.94	0.14	1.34	0.04	0.04	0	0.74	0.008	–	-	
	L004-X1	-	-	-	-	-	-	-	-	-	−27.8	−27.7	
	L004-X1	-	-	-	-	-	-	-	-	-	−28.2	−29.3	
	L004-X1	-	-	-	-	-	-	-	-	-	−28.4	−28.5	
	L4	P_2m	97.5	0.15	1.01	0.02	0.03	0	0.72	0.007	-	-	
	L4	P_2m	98.45	0.94	0.44	0.02	0	0	0.01	0.0001	-	-	
	L4	-	-	-	-	-	-	-	-	-	−27.7	−26.3	
	L4	-	-	-	-	-	-	-	-	-	−28.8	−28.4	
	L4	-	-	-	-	-	-	-	-	-	−28.8	−25.2	
	L16	P_2m	97.42	0.14	0.92	0.68	0.02	0.01	0.82	0.008	−28.8	−28.4	
	L16	-	-	-	-	-	-	-	-	-	−27.7	−26.3	
	L17	P_2q	97.16	0.1	1.38	0.96	0.04	0.01	0.37	0.004	−28.3	−25.2	

Note: GSI = 100 × $H_2S/(H_2S + CH_4 + C_2H_6 + C_3H_8)$.

5 Discussion

5.1 Origins of natural gas

5.1.1 Crude oil cracking gas or kerogen cracking gas

Oil-type gas can be derived from oil cracking or kerogen cracking, whereas the coal-type gas is mainly derived from the kerogen cracking. Therefore, it is necessary to judge the organic matter type of its source rocks before judging the genetic mechanism of natural gas. The crossplot of $\delta^{13}C_1$ versus $\delta^{13}C_2$ shows that the natural gas from the Hewangchang Area is oil-type gas and the natural gas from the Shuangyushi and Jiulongshan areas is the mixture of oil-type gas and coal-type gas (Figure 4). The crossplots of ln (C_1/C_2) versus $\delta^{13}C_1$ and ln (C_1/C_2) versus $\delta^{13}C_2$ can be used to distinguish the oil cracking gas and kerogen cracking gas (Liu et al., 2018). According to the crossplots, the natural gas from the Hewangchang Area is oil cracking gas, and the natural gas from the Shuangyushi and Jiulongshan areas is not typical oil cracking gas (Figure 5), which may be influenced by mixture with natural gas generated by humic kerogen cracking.

Some nonhydrocarbon gas can also indicate the origin of natural gas (Wang et al., 2018; Xiao et al., 2021). For example, natural gas generated by kerogen cracking is usually characterized by higher N_2 content than those generated by crude oil cracking. Kerogen in argillaceous rocks contains more nitrogen compounds than the crude oil, so under pyrolysis reactions, the denitrification of the kerogen can result in high N_2 contents in the kerogen cracking gas (Chen et al., 2000; Wang et al., 2018). The Devonian natural gas in the Northwestern Sichuan Basin is the typical crude oil cracking gas, whose N_2 and CO_2 contents are very low, less than 2.4% (Li et al., 2019). However, the Sinian natural gas in the southwestern Sichuan Basin is the typical kerogen cracking gas, which has high N_2 and CO_2 contents of more than 4% (Yin et al., 2001). The natural gas from the Shuangyushi, Hewanchang and Jiulongshan areas are all characterized by low N_2 and CO_2 contents, ranging from 0 to 1.43% and from 0 to 3.79%, respectively (Figure 6), which indicates that the natural gas from the above three areas were generated by crude oil cracking.

According to the above discussion, we suggest that the natural gas from the Hewanchang area is oil cracking gas, while the natural gas from the Shuangyushi and Jiulongshan areas is a mixture of oil cracking gas and humic kerogen cracking gas.

5.1.2 Originating from the lower cambrian source rocks or the upper-middle permian source rocks

There exist multiple sets of source rocks in the Sichuan Basin (Wei et al., 2018; Xu et al., 2018; Zheng et al., 2019), but considering the distribution and organic matter abundance, the Lower Cambrian and Upper-Middle Permian source rocks are the major source rocks for the natural gases in the Northwestern Sichuan Basin (Hu et al., 2021). Carbon isotopic composition of kerogen can indicate the type of organic matter (Kotarba and Clayton, 2003; Misz-Kennan and Fabianska, 2011). In general, the sapropelic kerogen has $\delta^{13}C_{kerogen}$ values less than −28‰, the mixed kerogen has $\delta^{13}C_{kerogen}$ values between −28‰ and −26‰, while the humic kerogen has $\delta^{13}C_{kerogen}$ values greater than −26‰ (Borjigen et al., 2014; Li et al., 2015a). The $\delta^{13}C_{kerogen}$ values of the ϵ_1q source rocks range from −38.7‰ to −34.9‰ (avg. −36.5‰), implying the sapropelic kerogen type (Table 2; Figure 7). The $\delta^{13}C_{kerogen}$ values of the P_2q and P_2m source rocks range from −29.2‰ to −24.2‰ (avg. −26.5‰), implying that they mainly contain the mixed kerogen (Table 2; Figure 7). However, the $\delta^{13}C_{kerogen}$ values of the P_3l source rocks range from −26.1‰ to −24.8‰ (avg. −26.9‰), implying humic kerogen type, which is consistent with the lithology of coal measure (Table 2; Figure 7). The methane $\delta^{13}C$ value of natural gas is affected by maturity, while the ethane carbon isotopes have a relatively strong inheritance from parent material type (Stahl, 1977; Li et al., 2019). Therefore, ethane carbon isotopes of natural gas are usually used to indicate the origin of natural gas. Ethane carbon isotopes can be affected by thermochemical sulphate reduction of sulphate minerals by hydrocarbons at elevated temperatures (Liu et al., 2014; Li et al., 2015b; Gong et al., 2018; Wu et al., 2019). The GSI value of 0.01 was proposed as the threshold of TSR (Liu et al., 2013, 2019) and the GSI values of natural gas in the Permian reservoirs of the Northwestern Sichuan Basin is less than 0.01 (Table 1), so the natural gas has not undergone TSR, which cannot affect the ethane carbon isotopes.

The $\delta^{13}C_2$ values of natural gas samples in the Hewanchang area range from −36.7‰ to −31.5‰, similar to the $\delta^{13}C_{kerogen}$ values of the ϵ_1q source rocks (Figures 4, 7), implying the natural gases mainly originate from the ϵ_1q source rocks. The $\delta^{13}C_2$ values of natural gas samples in the Shuangyushi area range from −28.6‰ to −25.9‰, similar to the $\delta^{13}C_{kerogen}$ values of the P_2q and P_2m source rocks (Figures 4, 7), implying the natural gases mainly originate from the Upper Permian source rocks, but the contribution from P_3l source rocks cannot be excluded only by carbon isotope data. The $\delta^{13}C_2$ values of natural gas samples in the Jiulongshan area have a relatively wide range compared to those in the Shuangyushi area, from −29.3‰ to −25.2‰, which is similar to the $\delta^{13}C_{kerogen}$ values of the P_2q, P_2m and P_3l source rocks (Figures 4, 7), indicating that the natural gases mainly originate from the above three sets of source rocks.

Biomarker analysis is an effective method for determining the origin of hydrocarbon (Chen et al., 2018; Adriana et al., 2020; Schwangler et al., 2020). The relative content of steranes can indicate the origins of organic matter (Li et al., 2022). The C_{27} sterane are mainly originated from lower aquatic organisms and algal organic matter, the C_{28} sterane are mainly related to specific

TABLE 2 Carbon isotopes of source rock samples from different tratigraphic intervals.

Series	Formation	Lithology	$\delta^{13}C$/‰
Lower Cambrian	Qiongzhusi	shale	−36.3
Lower Cambrian	Qiongzhusi	shale	−37.6
Lower Cambrian	Qiongzhusi	shale	−38.7
Lower Cambrian	Qiongzhusi	shale	−37.2
Lower Cambrian	Qiongzhusi	shale	−36.7
Lower Cambrian	Qiongzhusi	shale	−36.9
Lower Cambrian	Qiongzhusi	shale	−35.1
Lower Cambrian	Qiongzhusi	shale	−36.7
Lower Cambrian	Qiongzhusi	shale	−35.6
Lower Cambrian	Qiongzhusi	shale	−35.8
Lower Cambrian	Qiongzhusi	shale	−34.9
Middle Permian	Qixia	marlstones	−24.2
Middle Permian	Qixia	marlstones	−25.2
Middle Permian	Qixia	marlstones	−27.4
Middle Permian	Maokou	marlstones	−27.2
Middle Permian	Maokou	marlstones	−28.3
Middle Permian	Maokou	marlstones	−29.2
Upper Permian	Longtan	coal	−25.2
Upper Permian	Longtan	coal	−25.6
Upper Permian	Longtan	coal	−26.1
Upper Permian	Longtan	coal	−24.8

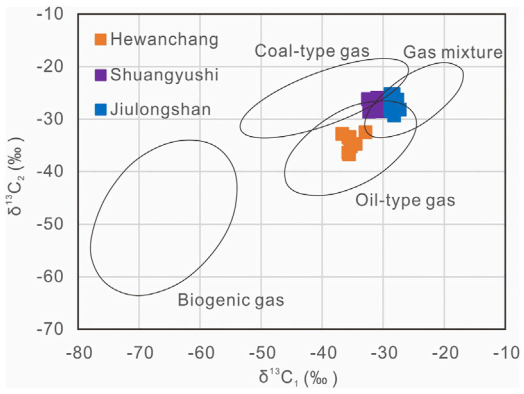

FIGURE 4
Cross-plot of $\delta^{13}C_1$ vs. $\delta^{13}C_2$ for natural gas samples from different areas to indicate the genetic types and origins of natural gas. The genetic types of natural gas are described in Liu et al., 2019.

phytoplankton such as diatoms, while the C_{29} sterane are mainly associated with higher plants as well as microalgae and blue-green algae (Huang and Meinschein, 1979; Grantham and Wakefield, 1988; Li et al., 2022). The Gam/C_{31}H and Ts/Tm ratios are the common biomarker parameters for oil-source correlation, which can indicate the salinity of water body and lithology respectively (Peters, et al., 2005). Li et al. (2022) analyzed the origins of Permian natural gas in different belts of the Northwest Sichuan Basin by the above biomarker characteristics of source rocks and Permian solid bitumen. The solid bitumen in the thrust nappe belt has abundant C_{29} steranes and large Gam/C_{31}H and Ts/Tm values, which resembles to those of theϵ_1q source rocks (Figures 8A,B), indicating that the natural gas in the thrust nappe belt is originated from theϵ_1q source rocks. The solid bitumen in the thrust front belt and unfaulted belt has both abundant C_{27} and C_{29} steranes and small Gam/C_{31}H and Ts/Tm ratios (Figures 8A,B), which resembles to those of the P_2q and P_2m source rocks, indicating that the natural gas in the thrust front belt and unfaulted belt is originated from the P_2q and P_2m source rocks. These results are basically consistent with those obtained by carbon isotope correlation.

5.2 Hydrocarbon accumulation process

Accurate determination of hydrocarbon charging time is the key to study hydrocarbon generation history and accumulation process. Fluid inclusion is one of the most common and effective methods to determine hydrocarbon charging period and time (Ni et al., 2016; Li et al., 2021; Pang et al., 2021). Chen et al. (2019b) found that the homogenization temperatures of brine inclusions associated with hydrocarbon inclusions in the reservoirs of the Shuangyushi Area are mainly distributed at 140–150°C and 160–170°C (Figure 9), indicating two stages of hydrocarbon charging. The GOI value in the first stage is larger than that in the second stage, indicating more hydrocarbons charged in the first stage. Combined with the burial and thermal history, it can be seen that the first hydrocarbon charging event occurred at late Triassic, while the second hydrocarbon charging event occurred at Early-Middle Jurassic (Figure 10).

The tectonic evolution of the Northwestern Sichuan Basin controlled the whole process of hydrocarbon accumulation, and combined the tectonic evolution history, the hydrocarbon accumulation process in the Northwestern Sichuan Basin can be divided into the following three stages (Figure 11).

5.2.1 Crude oil charging stage

In the late indosinian period, the slip nappe structure in the Northwestern Sichuan Basin was deformed, and a large-scale (large fault block) thrust nappe structure was formed under the control of the slip layer. At this time, the Lower Cambrian and the Upper-Middle Permian source rocks had entered the mature stage and the ϵ_1q, P_2q and P_2m source rocks generated large amounts of oils, while the P_3l source rocks of coal measures can only generate a certain amount of natural gas. Due to the existence of large thrust faults in the thrust nappe belt, the oil generated from the ϵ_1q source rocks can migrated along the thrust faults to the overlying reservoirs. However, there is few faults in the thrust front belt and unfaulted belt, so the Permian

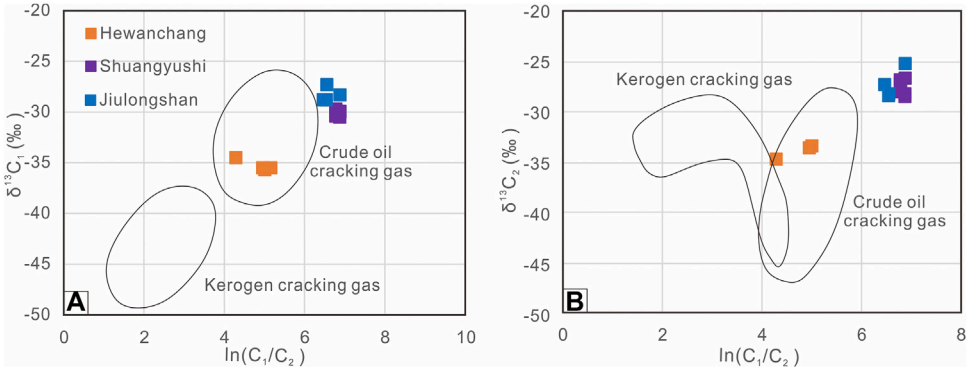

FIGURE 5
Cross-plots of ln (C_1/C_2) vs. $\delta^{13}C_1$ **(A)** and ln (C_1/C_2) vs. $\delta^{13}C_2$ **(B)** for natural gas samples from different areas to indicate the genetic types of natural gas. The distribution ranges of different genetic types of natural gas are referred to Liu et al. (2018).

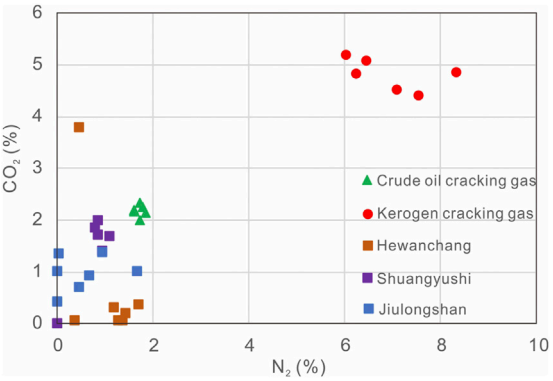

FIGURE 6
Cross-plot of N_2 vs. CO_2 for natural gas samples from different areas, showing the genetic types of natural gas. Samples of crude oil cracking gas and kerogen cracking gas are according to Li et al. (2019) and Yin et al. (2001), respectively.

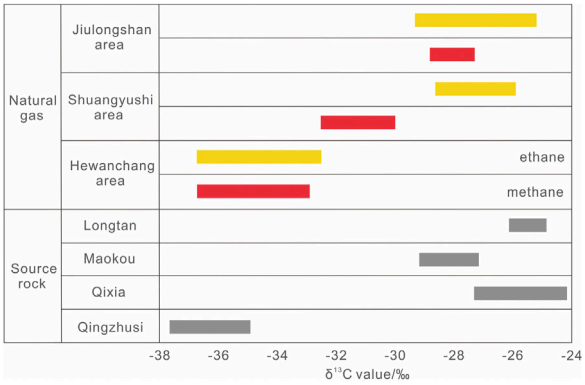

FIGURE 7
Carbon isotopes of source rock samples from different stratigraphic intervals and natural gas samples from different areas to indicate the origins of natural gas.

reservoirs there can only receive the oils and gas generated from the Upper-Middle Permian source rocks.

5.2.2 Oil cracking stage

In the Yanshanian period, the nappe further extends southeast. With the increase of the buried depth, the formation temperature increases continuously, resulting to the crude oil cracking to generate natural gas. The newly generated natural gas migrated a short distance to accumulate in the appropriate traps.

5.2.3 Gas reservoir adjustment stage

During the Himalayan period, with the continuous advance of the Longmen Mountain fold belt toward the passive margin, the strata in the Northwestern Sichuan Basin suffered severe deformation, resulting to the adjustment and destruction of large amounts of traps. The gas reservoirs were destroyed in the Kuangshanliang Area and went through large-scale adjustment in the other areas.

5.3 Main factors controlling the natural gas accumulation

5.3.1 Distribution of thrust faults

Faults can transport the hydrocarbons generated by the source rocks in deep layers to the reservoirs in shallow layers, and are the most important vertical migration pathways for hydrocarbons (Li et al., 2021). The faults and the associated fractures control the migration and subsurface location of hydrocarbon in carbonate and evaporate lithologies (Ameen, 2003; Lunn et al., 2008; Zhang et al., 2022). During the

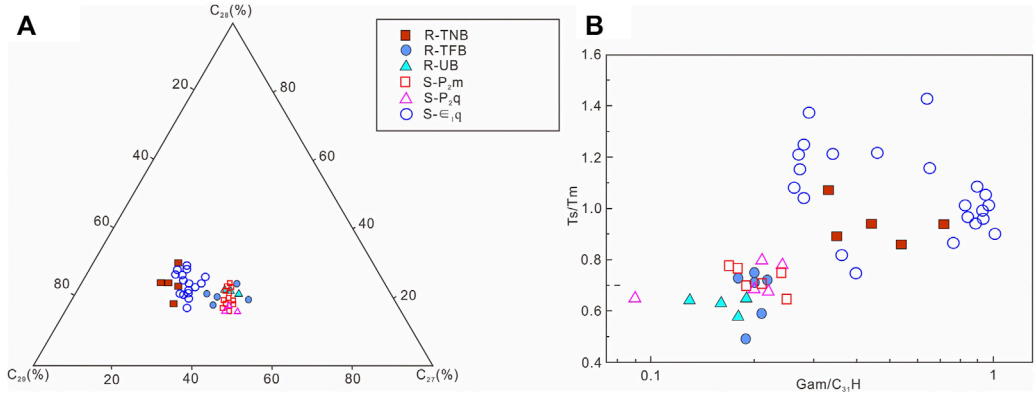

FIGURE 8
Biomarker characteristics for source rocks in different stratigraphic intervals and reservoir solid bitumen in different structural belts for determining the origins of natural gas (modified by Li et al., 2022). **(A)** Ternary plot of C_{27}–C_{28}–C_{29} steranes. **(B)** Cross plot of Gam/C_{31}H vs. Ts/Tm.

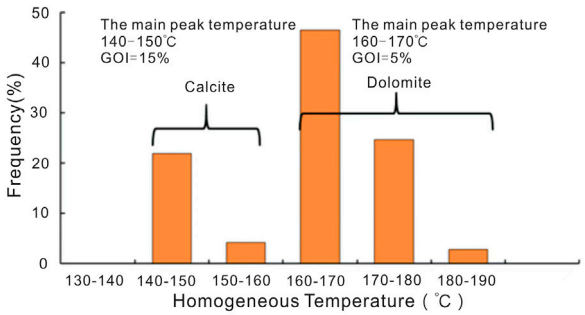

FIGURE 9
Homogenization temperature distribution of brine inclusions associated with hydrocarbon inclusions in the gas reservoirs of the Shuangyushi area (According to Chen et al., 2019b).

Indo–Yanshanian orogeny, under the influence of the large-scale subduction of the adjacent orogenic belt into the basin, a huge horizontal compressive stress field formed in the Northwestern Sichuan Basin (Gu et al., 2016; Li B. et al., 2020), creating large amounts of thrust faults. With the decreasing of the compressional stress from the thrust nappe belt to the thrust front belt and the unfaulted belt, the number and size of thrust faults decrease in the same order (Figures 3, 11).

The Hewanchang area is located in the thrust front belt, and develops many large thrust faults which extend down through the Cambrian strata and up to the Triassic and overlying strata. These thrust faults are favorable vertical migration paths for hydrocarbons generated by the ϵ_1q source rocks to enter the Permian reservoirs (Figure 11). Therefore, the natural gases in the Hewanchang area originate from the ϵ_1q source rocks. The Shuangyushi area is located in the thrust front belt. Although some thrust faults develop there, few of them extend down to the Cambrian strata. Therefore, hydrocarbons generated by theϵ_1q source rocks cannot migrate upward to the Permian reservoirs, which result to the fact that the natural gases in the Shuangyushi area mainly originate from the P_2q, P_2m and P_3l source rocks (Figure 11). However, the Jiulongshan area is located in the unfaulted belt and few thrust faults develop there. Therefore, the Permian reservoirs in the Jiulongshan area can only receive the hydrocarbons generated by the P_2q, P_2m and P_3l source rocks (Figure 11). According to the above discuss, it is the distribution of thrust faults that controls the hydrocarbon origins in different areas.

5.3.2 Preservation condition

The marine basins of China are usually located in the plates with small scale. Affected by multi-stage and multi-direction compressional tectonic movement such as the paleo-Asian ocean tectonic domain, western Pacific tectonic domain and Tethys tectonic domain, these basins are characterized by old age, multi-cycle evolution, complex basin-mountain structure, multi-period activity and poor stability, which makes the preservation condition an indispensable key factor for the large accumulation of hydrocarbons in the marine basins of China (Jia et al., 2006; Liu et al., 2011; Zhao et al., 2015). The Sichuan Basin is a typical marine basin during the Sinian to the Middle Triassic in China and the Northwestern Sichuan Basin is located in the transition region between the basin and mountain, so intense tectonic movement during the Himalayan orogeny caused the stratum deformation, fragmentation and denudation, which make a challenge for hydrocarbon preservation (Luo et al., 2020).

The Hewanchang area is in the thrust nappe belt adjacent to the thrust front belt. Although the stratum there were lifted up during the Himalayan orogeny, the regional caprocks of the thick shale in the Longtan Formation of the Upper Permian and the gypsum rocks in the Lower-Middle Triassic suffered little or no denudation and still owned strong sealing ability (Figure 11) (Luo

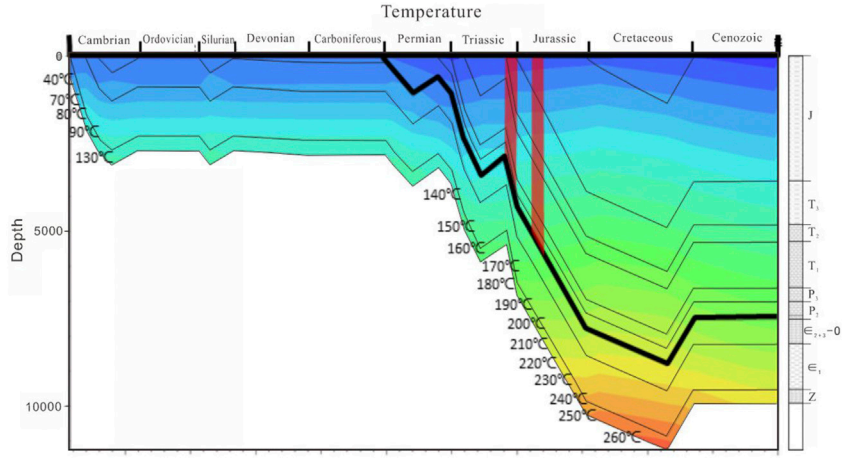

FIGURE 10
Burial and thermal history of the Northwestern Sichuan Basin to show the hydrocarbon charging stage and time.

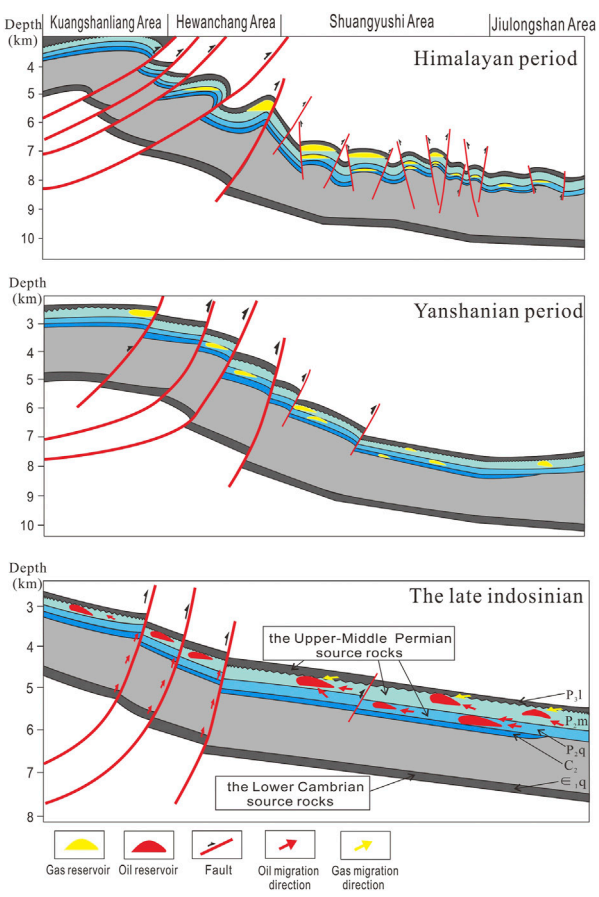

FIGURE 11
Hydrocarbon accumulation process in different periods and in different areas of the Northwestern Sichuan Basin.

et al., 2020). Therefore, natural gases can be preserved well after accumulation in the Hewanchang area. However, in the Kuanshanliang area, which is in the thrust nappe belt adjacent to the Longmen Mountain fold-and-thrust system, intense tectonic movement caused the opening of large deep thrust faults and the serious denudation of the regional caprocks due to violent stratum uplift (Figure 11) (Chen X. Z. et al., 2019). These caused the destruction of trap integrity, and then resulted to the oxidation and degradation of hydrocarbons to form exposed oil sands, oil seedlings and bitumen (Li et al., 2020a, b). In addition, due to weak compressional stress during the Himalayan orogeny, the stratum in the Shuangyushi area of the thrust front belt and the Jiulongshan area in the unfaulted belt suffered little or no uplift (Figure 11), so the regional caprocks of the Upper Permian and the Lower-Middle Triassic had a strong sealing ability and the natural gases in the Permian reservoirs owned a good preservation condition. This can be verified by the fact that the pressure coefficients of the gas reservoirs in the Shuangyushi area range from 1.4 to 1.8 and those in the Jiulongshan area range from 1.8 to 2.0 (Chen X. Z. et al., 2019).

5.4 Implications for natural gas exploration

Foreland basins are very important petroliferous basins over the world and the basin-mountain transition regions are key areas for hydrocarbon exploration in the foreland basins. The above discuss clearly reveals that the distribution of thrust faults and the preservation condition are the main factors controlling the natural gas accumulation in the Northwestern Sichuan Basin, a typical basin-mountain transition region. The distribution of

thrust faults controls the natural gas origins in different areas and the preservation condition determines whether the gas reservoirs can survive to the present or not. Under the influence of the large-scale subduction of the adjacent orogenic belt into the basin, the Northwestern Sichuan Basin can be divided into three regions, and different regions own unique geological features and gas accumulate rules.

The thrust nappe belt develops many large thrust faults extending down through the Low Cambrian source rocks, so the natural gases mainly originate from the Lower Cambrian source rocks. The area adjacent to the Longmen Mountain fold-and-thrust system suffered the most intense compressional stress and the regional caprocks suffered the serious uplift and denudation. Therefore, the natural gases cannot be preserved well and this area is not worth exploring the natural gas. However, the regional caprocks in the area adjacent to the thrust front belt suffered little or no denudation, so the natural gases in this area can be preserved well and are worth being explored.

The thrust front belt and the unfaulted belt only develops a few or few thrust faults, which cannot transport enough gases generated by the Low Cambrian source rocks to the overlying reservoirs. Therefore, the natural gases in the above two regions mainly originate from the Upper-Middle Permian source rocks. The regional caprocks there suffered little or no uplift and denudation, so the natural gases in the above two regions can be preserved well and are worth being explored.

6 Conclusion

The Northwestern Sichuan Basin is a typical basin-mountain transition region, with complex hydrocarbon accumulation rules. Under the influence of the large-scale subduction of the adjacent orogenic belt into the basin, the Northwestern Sichuan Basin can be divided into three structural belts: the unfaulted belt, the thrust front belt and the thrust nappe belt. Multiple sets of source rocks exist: Lower Cambrian source rocks containing sapropelic kerogen, Middle Permian source rocks containing mixed kerogen, and Upper Permian source rocks containing humic kerogen. The natural gas in the thrust nappe belt were mainly crude oil cracking gas, while the natural gas in the thrust front belt and the unfaulted belt were a mixture of crude oil cracking gas and humic kerogen cracking gas. The distribution of thrust faults controls the natural gas origins in different regions. The natural gas in the thrust nappe belt developing many large thrust faults mainly originates from the Lower Cambrian source rocks, while the natural gas in the thrust front belt and the unfaulted belt only developing a few or few thrust faults mainly originates from the Upper-Middle Permian source rocks. The preservation condition determines whether the gas reservoirs can survive to the present. The natural gas has poor preservation conditions in the thrust nappe belt adjacent to the Longmen Mountain fold-and-thrust system, where the regional caprocks suffered serious denudation, so this area is not worth exploring for natural gas. However, the natural gas can be preserved well in the thrust nappe belt adjacent to the thrust front belt, the thrust front belt and the unfaulted belt, where the regional caprocks suffered little or no denudation, so these areas have good prospects for natural gas exploration.

Data availability statement

The original contributions presented in the study are included in the article/supplementary material, further inquiries can be directed to the corresponding author.

Author contributions

HX is the first author of this article, responsible for the preparation of the full text. FX directed the research work of this paper and served as the corresponding author. XF, JZ, WL, and CC provide data support for this study. YW and KZ were responsible for the data collation of the study.

Funding

This study was funded by the PetroChina Project. The authors sincerely thank the collaboration and enthusiastic support from staff in the Hangzhou Institute of Geology and Southwest Oil and Gas Field Company of PetroChina. The funder had the following involvement in the study: financial support, study design and collecting project data. The funder was not involved in data analysis and interpretation, the writing of this article or the decision to submit it for publication.

Conflict of interest

XF, JZ, and WL were employed by the company PetroChina. CC was employed by the company PetroChina Southwest Oil and Gas Field Company. YW was employed by the company CNPC.

The remaining authors declare that the research was conducted in the absence of any commercial or financial relationships that could be construed as a potential conflict of interest.

Publisher's note

References

Adriana, M., Santos, M., Caroline, A., Eliane, S., Martins, L. L., and Rene, R. (2020). Degradation-resistant biomarkers in the Pirambóia Formation tar sands (Triassic) and their correlation with organic facies of the Irati Formation source rocks (Permian), Paraná. Brazil. *J. S. Am. Earth Sci.* 104, 102873. doi:10.1016/j.jsames.2020.102873

Al-ameri, T. K., and Zumberge, J. (2012). Middle and upper jurassic hydrocarbon potential of the Zagross Fold belt, North Iraq. *Mar. Petroleum Geol.* 36 (1), 13–34. doi:10.1016/j.marpetgeo.2012.04.004

Ameen, M. (2003). Fracture and *in-situ* stress characterization of hydrocarbon reservoirs: Definitions and introduction. *Geol. Soc. Lond. Spec. Publ.* 209, 1–6. doi:10.1144/gsl.sp.2003.209.01.01

Borjigen, T., Qin, J., Fu, X., Yang, Y., and Lu, L. (2014). Marine hydrocarbon source rocks of the Upper Permian Longtan Formation and their contribution to gas accumulation in the northeastern Sichuan Basin, southwest China. *Mar. Petroleum Geol.* 57, 160–172. doi:10.1016/j.marpetgeo.2014.05.005

Chen, C., Zhang, J., and Luo, B. (2019). Middle triassic-paleozoic pressure chamber and hydrocarbon accumulation in northwestern Sichuan Basin. *Nat. Gas. Ind.* 39 (04), 37–47. doi:10.3787/j.issn.1000-0976.2019.04.005

Chen, S. J., Fu, X. W., and Shen, Z. G. (2000). Molecular nitrogen Genesis in natural gas and relationship with gas accumulation history in Tarim Basin. *Acta Sedimentol. Sin.* 18, 615–618. (in Chinese with English abstract). doi:10.14027/j.cnki.cjxb.2000.04.024

Chen, X., Hao, F., Guo, L., Wang, D., Yin, J., Yang, F., et al. (2018). Origin of petroleum accumulation in the chaheji-gaojiapu structural belt of the baxian sag, bohai bay basin, China: Insights from biomarker and geological analyses. *Mar. Pet. Geol.* 93, 1–13. doi:10.1016/j.marpetgeo.2018.02.010

Chen, X. Z., Li, W., Wang, L. N., Lei, Y., Yang, G., Zhang, B., et al. (2019). Structural geology and favorable exploration prospect belts in Northwestern Sichuan Basin, SW China. *Petroleum Explor. Dev.* 46 (2), 413–425. doi:10.1016/s1876-3804(19)60022-4

Decelles, P. G., and Gilest, K. A. (1996). Foreland basin systems. *Basin Res.* 8, 105–123. doi:10.1046/j.1365-2117.1996.01491.x

Deming, D., and Chapman, D. S. (1988). Inversion of bottom-hole temperature data; the Pineview Field, Utah-Wyoming thrust belt. *Geophysics* 53 (5), 707–720. doi:10.1190/1.1442504

Deng, J., Liu, M., Ji, Y., Tang, D., Zeng, Q., Song, L., et al. (2022). Controlling factors of tight sandstone gas accumulation and enrichment in the slope zone of foreland basins: The Upper Triassic Xujiahe Formation in Western Sichuan Foreland Basin, China. *J. Petroleum Sci. Eng.* 214, 110474. doi:10.1016/j.petrol.2022.110474

Gong, D., Li, J., Ablimit, I., He, W., Lu, S., Liu, D., et al. (2018). Geochemical characteristics of natural gases related to Late Paleozoic coal measures in China. *Mar. Petroleum Geol.* 96, 474–500. doi:10.1016/j.marpetgeo.2018.06.017

Grantham, P. J., and Wakefield, L. L. (1988). Variations in the sterane carbon number distributions of marine source rock derived crude oils through geological time. *Org. Geochem.* 12 (1), 61–73. doi:10.1016/0146-6380(88)90115-5

Gu, Z., Yin, J., Jiang, H., Zhang, B., Li, Q., Yuan, M., et al. (2016). Tectonic evolution from late sinian to early paleozoic and natural gas exploration in northwestern Sichuan Basin, SW China. *Petroleum Explor. Dev.* 43 (1), 1–12. doi:10.1016/s1876-3804(16)30001-5

Guo, R., Wang, Q., and Wang, J. (2021). Oil-source correlation and stages of reservoir formation of the Alade oilfield in the Northwestern Junggar Basin of China. *J. Northeast Petroleum Univ.* 45 (3), 54–61. doi:10.3969/j.issn.2095-4107.2021.03.006

Guo, X., Hu, D., Huang, R., Wei, Z., Duan, J., Wei, X., et al. (2020). Deep and ultradeep natural gas exploration in the Sichuan Basin: Progress and prospect. *Nat. Gas. Ind. B* 7 (5), 419–432. doi:10.1016/j.ngib.2020.05.001

He, D., and Jia, C. (2005). Thrust tectonics and hydrocarbon accumulation. *Petroleum Explor. Dev.* 32 (2), 55–62. doi:10.3321/j.issn:1000-0747.2005.02.013

Hu, G., He, F., Mi, J., Yuan, Y., and Guo, J. (2021). The geochemical characteristics, distribution of marine source rocks and gas exploration potential in the Northwestern Sichuan Basin, China. *J. Nat. Gas Geoscience* 6 (4), 199–213. doi:10.1016/j.jnggs.2021.07.004

Huang, W., and Meinschein, W. (1979). Sterols as ecological indicators. *Geochimica Cosmochimica Acta* 43 (5), 739–745. doi:10.1016/0016-7037(79)90257-6

Huo, F., Yang, X., and Wang, C. (2018). Characteristics and main controlling factors of the middle permian Maokou formation reservoir in northwestern Sichuan Basin, China. *J. Chengdu Univ. Technol. Sci. Technol. Ed.* 45 (1), 45–52. (in Chinese with English abstract). doi:10.3969/j.issn.1671-9727.2018.01.04

Jia, C. Z., He, D. F., Shi, X., Yang, G., and Zhang, C. (2006). Characteristics of China's oil and gas pool formation in latest geological history. *Sci. China (Series D)* 49 (9), 947–959. doi:10.1007/s11430-006-0947-7

Kotarba, M. J., and Clayton, J. L. (2003). A stable carbon isotope and biological marker study of Polish bituminous coals and carbonaceous shales. *Int. J. Coal Geol.* 55, 73–94. doi:10.1016/s0166-5162(03)00082-x

Li, B., Mei, W., and Li, Q. (2020a). Influence of tectonic evolution of foreland basin in Northwestern Sichuan Basin on Paleozoic marine hydrocarbon accumulation. *Nat. Gas. Geosci.* 31 (7), 993–1003. doi:10.11764/j.issn.1672-1926.2020.02.008

Li, C. Z., Xu, G. S., Xu, F. H., Yu, Q., and Liang, H. (2021). A model for faults to link the Neogene reservoirs to the Paleogene organic-rich sediments in low-relief regions of the south Bohai Sea, China. *J. Petroleum Sci. Eng.* 200, 108360. doi:10.1016/j.petrol.2021.108360

Li, P., Hao, F., Guo, X., Zou, H., Yu, X., and Wang, G. (2015b). Processes involved in the origin and accumulation of hydrocarbon gases in the Yuanba gas field, Sichuan Basin, southwest China. *Mar. Petroleum Geol.* 59, 150–165. doi:10.1016/j.marpetgeo.2014.08.003

Li, P., Hao, F., Zhang, B., Zou, H., Yu, X., and Wang, G. (2015a). Heterogeneous distribution of pyrobitumen attributable to oil cracking and its effect on carbonate reservoirs: Feixianguan Formation in the Jiannan gas field, China. *Am. Assoc. Pet. Geol. Bull.* 99, 763–789. doi:10.1306/11051414018

Li, Q., Li, B., Mei, W., and Liu, Y. (2022). Genesis and sources of natural gas in fold-and-thrust belt: The Middle Permian in the NW Sichuan Basin. *Mar. Petroleum Geol.* 140, 105638. doi:10.1016/j.marpetgeo.2022.105638

Li, W., Yu, Z., Wang, X., Lu, X., and Feng, Q. (2020c). Formation mechanisms of deep and ultradeep over pressure caprocks and their relationships with superlarge gas fields in the petroliferous basins of China. *Nat. Gas. Ind. B* 7 (5), 443–452. doi:10.1016/j.ngib.2020.09.002

Li, Y., Chen, S., Wang, Y., Qiu, W., Su, K., He, Q., et al. (2019). The origin and source of the Devonian natural gas in the Northwestern Sichuan Basin, SW China. *J. Petroleum Sci. Eng.* 181, 106259. doi:10.1016/j.petrol.2019.106259

Li, Y., Chen, S., Wang, Y., Su, K., He, Q., Qiu, W., et al. (2020b). Relationships between hydrocarbon evolution and the geochemistry of solid bitumen in the Guanwushan Formation, NW Sichuan Basin. *Mar. Petroleum Geol.* 111, 116–134. doi:10.1016/j.marpetgeo.2019.08.018

Liu, Q., Jin, Z., Wang, X., Yi, J., Meng, Q., Wu, X., et al. (2018). Distinguishing kerogen and oil cracked shale gas using H, C-isotopic fractionation of alkane gases. *Mar. Petroleum Geol.* 91, 350–362. doi:10.1016/j.marpetgeo.2018.01.006

Liu, Q., Wu, X., Wang, X., Jin, Z., Zhu, D., Meng, Q., et al. (2019). Carbon and hydrogen isotopes of methane, ethane, and propane: A review of genetic identification of natural gas. *Earth-Science Rev.* 190, 247–272. doi:10.1016/j.earscirev.2018.11.017

Liu, Q. Y., Worden, R. H., Jin, Z. J., Liu, W., Li, J., Gao, B., et al. (2014). Thermochemical sulphate reduction (TSR) versus maturation and their effects on hydrogen stable isotopes of very dry alkane gases. *Geochimica Cosmochimica Acta* 137, 208–220. doi:10.1016/j.gca.2014.03.013

Liu, Q. Y., Worden, R. H., Jin, Z. J., Liu, W., Li, J., Gao, B., et al. (2013). TSR versus non-TSR processes and their impact on gas geochemistry and carbon stable isotopes in Carboniferous, Permian and Lower Triassic marine carbonate gas reservoirs in the Eastern Sichuan Basin, China. *Geochimica Cosmochimica Acta* 100, 96–115. doi:10.1016/j.gca.2012.09.039

Liu, S., Deng, B., and Li, Z. (2011). The texture of sedimentary basin-orogenic belt system and its influence on oil/gas distribution: A case study from Sichuan basin. *Acta Petrol. Sin.* 27 (3), 621–635.

Lunn, R. J., Willson, J. P., Shipton, Z. K., and Moir, H. (2008). Simulating brittle fault growth from linkage of preexisting structures. *J. Geophys. Res.* 113 (B7), B07403. doi:10.1029/2007jb005388

Luo, B., Wen, L., and Zhang, Y. (2020). Differential gas accumulation process of the middle permian Qixia Formation, northwestern Sichuan Basin. *Oil gas Geol.* 41 (2), 393–406. doi:10.11743/ogg20200215

Macclay, K. R. (2004). Thrust tectonics and hydrocarbon systems. *AAPG Mem.* 82. doi:10.1306/M82813

Miao, Z., Pei, Y., Su, N., Sheng, S., Feng, B., Jiang, H., et al. (2022). Spatial and temporal evolution of the Sinian and its implications on petroleum exploration in the Sichuan Basin, China. *J. Petroleum Sci. Eng.* 210, 110036. doi:10.1016/j.petrol.2021.110036

Misz-Kennan, M., and Fabianska, M. J. (2011). Application of organic petrology and geochemistry to coal waste studies. *Int. J. Coal Geol.* 88, 1–23. doi:10.1016/j.coal.2011.07.001

Ni, Z. H., Wang, T. G., Li, M. J., Fang, R. H., Li, Q. M., Tao, X. W., et al. (2016). An examination of the fluid inclusions of the well RP3-1 at the Halahatang Sag in Tarim Basin, northwest China: Implications for hydrocarbon charging time and fluid evolution. *J. Petroleum Sci. Eng.* 146, 326–339. doi:10.1016/j.petrol.2016.04.038

Pang, Y., Shi, B., Guo, X., Zhang, X., Han, Z., Cai, L., et al. (2021). Source–reservoir relationships and hydrocarbon charging history in the central uplift of the south Yellow Sea basin (East Asia): Constrained by machine learning procedure and basin modeling. *Mar. Petroleum Geol.* 123, 104731. doi:10.1016/j.marpetgeo.2020.104731

Peters, K. E., Walters, C. C., and Moldowan, J. M. (2005). *The biomarker guide, biomarkers and isotopes in Petroleum exploration and Earth history*. Cambridge: Cambridge University Press.

Picha, F. J. (2011). Late orogenic faulting of the foreland plate: An important component of petroleum systems in orogenic belts and their forelands. *Am. Assoc. Pet. Geol. Bull.* 95 (6), 957–981. doi:10.1306/11191010006

Schwangler, M., Harris, N. B., and Waldron, J. W. F. (2020). Source rock characterization and oil-to-source rock correlation of a Cambrian -Ordovician fold-and-thrust belt petroleum system, Western Newfoundland. *Mar. Pet. Geol.* 115, 104283. doi:10.1016/j.marpetgeo.2020.104283

Stahl, W. J. (1977). Carbon and nitrogen isotopes in hydrocarbon research and exploration. *Chem. Geol.* 20, 121–149. doi:10.1016/0009-2541(77)90041-9

Wang, Q., Zhang, D. Y., and Wang, J. (2018). Hydrocarbon and nonhydrocarbon characteristics for comprehensive identification about kerogen pyrolysis gas and oil cracked gas. *Nat. Gas. Geosci.* 29, 1231–1239. (in Chinese with English abstract). doi:10.11764/j.issn.1672-1926.2018.07.003

Wei, G., Wang, Z., Li, J., Yang, W., and Xie, Z. (2018). Characteristics of source rocks, resource potential and exploration direction of Sinian-Cambrian in Sichuan Basin, China. *J. Nat. Gas Geoscience* 2 (5-6), 289–302. doi:10.1016/j.jnggs.2018.02.002

Wei, G., Yang, W., Liu, M., Xie, W., Jin, H., Wu, S., et al. (2020). Distribution rules, main controlling factors and exploration directions of giant gas fields in the Sichuan Basin. *Nat. Gas. Ind. B* 7 (1), 1–12. doi:10.1016/j.ngib.2020.01.001

Wei, Y., Yang, T., and Guo, S. (2019). Oil and gas resource potentials, exploration fields and favorable zones in foreland thrust belts. *China Pet. Explor.* 24 (1), 46–59.

Worden, R. H., Smalley, P. C., and Oxtoby, N. H. (1995). Gas souring by thermochemical sulfate reduction at 140°C. *AAPG Bull.* 79, 854–863. doi:10.1306/8D2B1BCE-171E-11D7-8645000102C1865D

Wu, A., Cao, J., and Zhang, J. (2021). Bedding-parallel calcite veins indicate hydrocarbon–water–rock interactions in the overmature Longmaxi shales, Sichuan Basin. *Mar. Petroleum Geol.* 133, 105303. doi:10.1016/j.marpetgeo.2021.105303

Wu, X., Liu, Q., Liu, G., and Ni, C. (2019). Genetic types of natural gas and gas-source correlation in different strata of the Yuanba gas field, Sichuan Basin, SW China. *J. Asian Earth Sci.* 181, 103906. doi:10.1016/j.jseaes.2019.103906

Xiao, D., Wen, L., Zhang, Y., Xie, C., Tan, X., and Cao, J. (2021). Natural gas accumulation in the basin–mountain transition zone, Northwestern Sichuan Basin, China. *Mar. Petroleum Geol.* 133, 105305. doi:10.1016/j.marpetgeo.2021.105305

Xu, Q., Qiu, N., Liu, W., Shen, A., and Wang, X. (2018). Thermal evolution and maturation of sinian and cambrian source rocks in the central Sichuan Basin, southwest China. *J. Asian Earth Sci.* 164, 143–158. doi:10.1016/j.jseaes.2018.06.015

Yin, C. H., Wang, T. D., Wang, S. Y., and Lin, F. (2001). Differences between Kerogen and oil cracked gases in Sinian reservoirs of Weiyuan and Ziyang area. *Acta Sedimentol. Sin.* 19 (1), 156–160. (in Chinese with English abstract). doi:10.14027/j.cnki.cjxb.2001.01.028

Zhang, L., Liao, Z., Long, K., Carpenter, B. M., Zou, H., and Hao, F. (2022). Fundamental constraints of lithologically controlled fault networks on gas migration and accumulation for fractured carbonates in the Western Sichuan Basin, China. *J. Petroleum Sci. Eng.* 208, 109502. doi:10.1016/j.petrol.2021.109502

Zhao, W. Z., Hu, S. Y., Liu, W., Wang, T., and Jiang, H. (2015). The multistaged "golden zones" of hydrocarbon exploration in superimposed petroliferous basins of onshore China and its significance. *Petroleum Explor. Dev.* 42 (1), 1–13. doi:10.1016/s1876-3804(15)60001-5

Zheng, T., Ma, X., Pang, X., Wang, W., Zheng, D., Huang, Y., et al. (2019). Journal of petroleum science and engineering organic geochemistry of the upper triassic T_3x^5 source rocks and the hydrocarbon generation and expulsion characteristics in Sichuan Basin, central China. *J. Petroleum Sci. Eng.* 173, 1340–1354. doi:10.1016/j.petrol.2018.10.070